GEOMETRY, VIBRATIONAL, NBO, MEP AND HOMO-LUMO ANALYSIS OF TETRAHYDROFURAN (THF) BASED ON DFT CALCULATIONS

Truong Tan Trung[1*], Nguyen Phuong Dong[2],
Lai Thi Hien[1], Le Thi Thu Thuy[1]
[1]Dong Nai Technology University, Dong Nai, Vietnam
[2]Department of Chemistry, Soongsil University, Seoul, Korea
Email: truongtantrung@dntu.edu.vn

ABSTRACT

In this paper, the density functional theoretical (DFT) computations were performed at the B3LYP level with the basis set 6-311++G(2d,2p) to derive the optimized geometry, vibrational wavenumbers. The fundamental vibrations were assigned on the basis of the potential energy distribution (PED) of the vibrational modes, calculated with VEDA program. In addition, the molecular orbital calculations, such as Nutural Bond Orbital (NBO), HOMO-LUMO energy gap and Molecular Electrostatic Potential (MEP) surfaces, were also performed with the same level of DFT. Effective second-order perturbation interaction energy E(2) connected with the interaction between electron donors and electron acceptors was determined by the NBO analysis. The energy gap of HOMO–LUMO orbitals ($\Delta E_{HOMO-LUMO}$) has been found 6.558 eV. Some essential vibrational characteristics namely C–H stretch, C–H scissoring and twisting of the molecule, have also been analyzed and compared with the previously reported ab initio data and with the experimental.

Keywords: Tetrahydrofuran, DFT, NBO, MEP, HOMO-LUMO.

1. INTRODUCTION

Density functional theory (DFT) is a quantum mechanical theory used in physics and chemistry to investigate the electronic structure of many-body systems; in particular atoms, molecules, and the condensed phases. According to this theory, the properties of a many-electron system can be determined by using functional, i.e. functions of another function, In the case of DFT, these are functionals of the spatially dependent electron density. Hence the name DFT comes to form the use of functional of the electron density. DFT is one of the most popular and versatile methods available in condensed-matter physics, computational physics, and computational chemistry [1].

Tetrahydrofuran (THF) is a prototype of heterocyclic five-member-ring structures with the formula $(CH_2)_4O$. The compound is classified as a heterocyclic compound, specifically a cyclic ether. It is a colorless, water-miscible organic liquid with low viscosity at standard temperature and pressure. THF has an odor similar to acetone. As one of the most polar ethers and having a wide liquid range it is a versatile solvent, which can be viewed as an oxygen-substituted cyclopentane. THF is of fundamental importance for biological studies, since this molecule constitutes the furanose ring in the backbone of certain carbohydrates and DNA/RDN. Thus, investigations on the molecular structure is necessary.

There are some experimental and theoretical studies on the geometrical structure of THF [2-4]. The theoretical studies used for calculations are very low level and do not show all the properties of the molecule. Therefore, this study aims to improve the vibrational spectra of the title molecule and indentifies the various modes with greater wavenumber accuracy. DFT calculations have been performed to support our wavenumber assignments and further study the theoretical determination of the optimized molecular geometries, MEP, HOMO-LUMO, and NBO analysis of the Tetrahydrofuran using the DFT method by employing B3LYP/6-311++G(2d,2p) basis sets. The experimental and theoretical results support each other, and the calculations are valuable for providing reliable insight into the vibrational spectra and molecular properties.

2. COMPUTATIONAL METHODS

The molecular structure of the title compound was fully optimized at the Density Functional Theory (DFT) level using a hybrid functional B3LYP (Becke's three-parameter exchange functional [5] combined with the Lee-Yang-Parr correlation functional [6] with the 6-311++G(2d,2p) basis set [7]. The natural bond orbital (NBO) calculations [8] were performed using GenNBO 5.G program as implemented in the Gaussian 09 package at the DFT/B3LYP/6-311++G(2d,2p) level. In addition, molecular electrostatic potential (MEP) of Tetrahydrofuran was investigated using theoretical calculations [9]. All calculations were carried out using the GAUSSIAN 09 program [10]. The calculated results were visualized via GaussView 6.0 program [11].

3. RESULTS AND DISCUSSION

3.1. Opitimzed geometry

Tetrahydrofuran (THF) was subjected to geometry optimization in the potential energy surfaces. The optimized geometry results showed that the title molecule belongs to C_1 point group symmetry. The optimized molecular structure of the THF with the atom nunbering scheme adopted in the present study is presented in Figure 1. The optimized structural parameters of THF are calculated by DFT/B3LYP level with basis set 6-311++G(2d,2p), MP2 (the second-order Moller-Plesset perturbation theory) level with basis set aug-cc-pVTZ and experimental have been compared in Table 1. It can be found from Table 1 that the theoretical values of Tetrahydrofuran exactly coincide with the experimental values [12] in both two methods. In the literature, bond lengths for C-C (1.528-1.537 Å, B3LYP/6-311+G**) [13] is close to the value reported in this paper. But slightly higher values of 1.443-1.446 Å (for (C-O)). This may be due to shifting of charge in interaction of THF with water molecule.
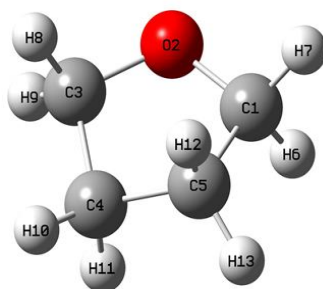
Figure 1. The optimized molecular structure and atom numbering scheme
adopted for Tetrahydrofuran at the B3LYP/6-311++G(2d,2p) level

Table 1. Optimized geometrical parameters (bond lengths and angles)
for Tetrahydrofuran calculated at different levels of theory

Parameters [a]	B3LYP	MP2	Experimental [b]
	6-311++G(2d,2p)	aug-cc-pVTZ	
R (1, 2)	1.436	1.434	1.438
R (2, 3)	1.436	1.434	
R (1, 5)	1.529	1.523	1.516
R (3, 4)	1.529	1.523	
R (4, 5)	1.535	1.527	1.536
R (1, 6)	1.095	1.094	1.094
R (1, 7)	1.090	1.089	-
R (3, 8)	1.095	1.094	-
R (3, 9)	1.090	1.089	-
R (4, 10)	1.089	1.088	-
R (4, 11)	1.091	1.091	-
R (5, 12)	1.091	1.091	-
R (5, 13)	1.089	1.088	-
A (1, 2, 3)	110.0	109.3	109.9
A (2, 1, 5)	106.3	106.1	-
A (2, 3, 4)	106.3	106.1	
A (1, 5, 4)	101.9	101.1	-
A (3, 4, 5)	101.9	101.1	
A (6, 1, 7)	108.4	108.8	-
A (8, 3, 9)	108.4	108.8	
A (10, 4, 11)	108.1	108.8	-
A (12, 5, 13)	108.1	108.8	

Note: Bond lengths in Å, angles in degrees
[a] Calculated with 6-311++G(2d,2p) and aug-cc-pVTZ basis sets. See Figure 1 for atoms numbering.
[b] Take from Ref. [12].

3.2. Vibrational analysis

The frequencies were calculated in the harmonic approximation at the B3LYP/6-311++G(2d,2p) level of theory. Tetrahydrofuran has 13 atoms with 33 normal modes of vibrational are active. The assignment of the fundamental vibrational modes is proposed on the basis of potential energy distribution (PED) using the VEDA 4 program [14]. The detailed assignments along with the vibration frequencies and the percentage of PED are summarized in Table 2. Here we are discussing important modes only. The experimental and calculated FT-IR spectra are presented in Figure 2 for comparison purposes.
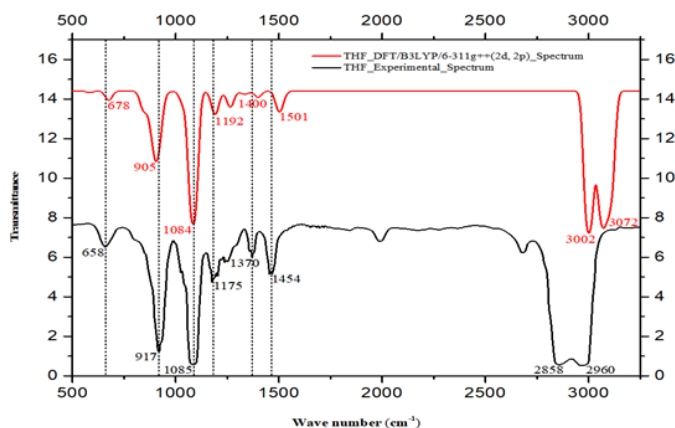
Figure 2. Experimental and calculated FT-IR spectra of Tetrahydrofuran

3.2.1. Spectral region between 3200 and 2800 cm^{-1}

For all aromatic compounds, the C–H stretching vibrations are observed in the region 3200-3000 cm^{-1} [15,16]. In the present study, the bands at 3072, and 3002 cm^{-1} are attributed to the C–H stretching mode which is clearly displayed similarities in peak positions with the experimental. The PED associated with the C–H mode of Tetrahydrofuran as given in Table 2.

Table 2. Calculated vibrational frequencies and mode assignments calculated frequencies of Tetrahydrofuran at B3LYP/6-311++G(2d,2p) level

No.	Frequencies Exp. (cm^{-1}) [a]	Frequencies Cal_DFT/B3LYP/6-311g++(2d,2p) (cm^{-1})	[b] Assignments based on PED calculations
1	658	678	16% ν (C$_4$-C$_3$) + 16% ν (C$_5$-C$_1$) + 69% β (C$_3$-O$_2$-C$_1$)
2	917	905	50% ν (C$_4$-C$_3$) + 50% ν (C$_5$-C$_1$)
3	1085	1084	36% ν (O$_2$-C$_1$) + 36% ν (O$_2$-C$_3$) + 14% β (C$_5$-C$_1$-O$_2$) + 14% β (C$_4$-C$_3$-O$_2$)
4	1175	1192	21% β (C$_5$-C$_1$-O$_2$) + 28% β (H$_{10}$-C$_4$-C$_5$) + 21% β (C$_4$-C$_3$-O$_2$) + 30% δ (H$_{13}$-C$_5$-C$_4$-C$_3$)
5	1370	1400	26% δ (H$_6$-C$_1$-O$_2$-C$_3$) + 24% δ (H$_7$-C$_1$-O$_2$-C$_3$) + 26% δ (H$_8$-C$_3$-O$_2$-C$_1$) + 24% δ (H$_9$-C$_3$-O$_2$-C$_1$)
6	1454	1501	49% β (H$_{11}$-C$_4$-H$_{10}$) + 51% β (H$_{13}$-C$_5$-H$_{12}$)
7	2858	3002	50% ν (C$_1$-H$_6$) + 50% ν (C$_3$-H$_8$)
8	2960	3072	50% ν (C$_1$-H$_7$) + 50% ν (C$_3$-H$_9$)

[a] NIST database: https://webbook.nist.gov/cgi/cbook.cgi?ID=C109999&Type=IR-SPEC&Index=1).
[b] Abbreviations: ν, β, and δ denote stretching, in-plane bending and torsion modes, respectively.

3.2.2. Spectral region between 1500 and 800 cm^{-1}

The aromatic C–H in-plane bending vibrations are observed in the region from 1300 to 1000 cm^{-1} [17]. Accordingly, the C–H in-plane bending of Tetrahydrofuran is observed at 1192 cm^{-1}. Besides, the results listed in Table 2 show that one of the strong vibration in the

infrared spectrum of Tetrahydrofuran is found at 1084 cm^{-1}. The theoretical scaled wavenumber of these mode is found to be in excellent agreement with the experimental wavenumber (1085 cm^{-1}). This is assigned to the antisymmetric C–O which the PED contribution to these modes is 36%.

3.2.3. Spectral region below 800 cm^{-1}

The region below 800 cm^{-1} is mostly dominated by in-plane and out-of-plane ring vibration. In this region, the band observed at 678 cm^{-1} is assigned to ring in-plane bending mode of C–O–C. The PED contribution to these modes is 69%.

3.3. NBO analysis

NBO analysis has been performed on the THF molecule at B3LYP/6-311++G(2d,2p) level of theory. Natural bond orbital (NBO) analysis is also useful too for understanding delocalization of electron density from occupied Lewis-type (donor) NBO to properly unoccupied non-Lewis type (acceptor) NBO within the molecule. The interaction between bonding and anti-bonding molecular orbitals can be quantitatively described in terms of NBO approach that is expressed by means of second-order perturbation interaction energy E(2). This energy represents the esimate of the off-diagonal NBO Fock matrix element. The stabilization energy E(2) associated with i (donor) $\rightarrow$ j (acceptor) delocalization is estimated from the secon-order perturbation approach as given below [8, 18].

$$E(2) = \Delta E_{ij} = q_i \frac{F^2(i, j)}{\varepsilon_j - \varepsilon_i}$$

Where q_i is the donor orbital occupancy, ε_i and ε_j are diagonal elements (orbital energies) and F(i,j) is the off-diagonal Fock matrix element.

Higher the E(2) value, the more intensive is the interaction between electron donors and electron acceptors, i.e., the more donating tendency from electron donors to electron acceptors and greater is the extent of conjugation of the whole system. Delocalization of electron density between occupied Lewis-type (bond or lone pair) NBO orbitals and formally unoccupied (antibond or Rydgerg) non-Lewis NBO orbitals correspond to a stabilizing donor-acceptor interaction. NBO analysis has been performed on the THF molecule at B3LYP/6-311++G(2d,2p) level of theory.

Table 3 show the most relevant hyper-conjugative interactions for the title compound performed by NBO analysis. The hyper-conjugative interactions are formed by the orbital overlap between π (O) bond orbital to π* (C–C), π* (C–H) anti-bonding orbital, which results in intra-molecular charge transfer causing the stabilization of the system. As can be seen in Table 3, the bond paid donor orbital π O $\rightarrow$ π* (C–C(H)) give more energy stabilization than σ (C– C(H)) $\rightarrow$ σ* (C– C(H), σ (C– H) $\rightarrow$ σ* (O– C). The energy value of the interactions π O(2) $\rightarrow$ π* C(1) – H(6) and π O(2) $\rightarrow$ π* C(3) – H(8) are 28.3 KJ mol^{-1}, indicating that these interactions produce a great stabilization in the molecule.

Table 3. Second-order perturbation theory analysis of the Fock matrix
for Tetrahydrofuran caluclated by the NBO method

Interaction (donor → acceptor) [a]	E(2) [b]	
	(Kcal mol^{-1})	(KJ mol^{-1})
π O(2) → π* C(1) – C(5)	2.47	10.3
π O(2) → π* C(1) – H(6)	6.77	28.3
π O(2) → π* C(1) – H(7)	4.70	19.7
π O(2) → π* C(3) – C(4)	2.47	10.3
π O(2) → π* C(3) – H(8)	6.77	28.3
π O(2) → π* C(3) – H(9)	4.70	19.7
σ C(1) – C(5) → σ* C(4) – C(5)	0.61	2.6
σ C(1) – C(5) → σ* C(4) – H(10)	2.20	9.2
σ C(1) – C(5) → σ* C(5) – H(13)	0.51	2.1
σ C(1) – H(6) → σ* O(2) – C(3)	1.10	4.6
σ C(1) – H(6) → σ* C(5) – H(12)	2.25	9.4
σ C(1) – H(6) → σ* C(5) – H(13)	0.57	2.4
σ C(1) – H(7) → σ* O(2) – C(3)	1.83	7.7
σ C(1) – H(7) → σ* C(4) – C(5)	1.44	6.0
σ C(1) – H(7) → σ* C(5) – H(12)	0.66	2.8
σ O(2) – C(3) → σ* C(4) – H(10)	0.90	3.8
σ C(3) – C(4) → σ* C(4) – C(5)	0.61	2.6
σ C(3) – C(4) → σ* C(4) – H(10)	0.51	2.1
σ C(3) – C(4) → σ* C(5) – H(13)	2.20	9.2
σ C(3) – H(8) → σ* C(1) – O(2)	1.10	4.6
σ C(3) – H(8) → σ* C(4) – H(10)	0.57	2.4
σ C(3) – H(8) → σ* C(4) – H(11)	2.25	9.4
σ C(3) – H(9) → σ* C(1) – O(2)	1.83	7.7
σ C(3) – H(9) → σ* C(4) – C(5)	1.44	6.0
σ C(3) – H(9) → σ* C(1) – H(11)	0.66	2.8
σ C(4) – C(5) → σ* C(1) – O(2)	1.86	7.8
σ C(4) – C(5) → σ* C(1) – C(5)	0.52	2.2
σ C(4) – C(5) → σ* C(1) – H(7)	1.66	6.9
σ C(4) – C(5) → σ* O(2) – C(3)	1.86	7.8
σ C(4) – C(5) → σ* C(3) – C(4)	0.52	2.2
σ C(4) – C(5) → σ* C(3) – H(9)	1.66	6.9
σ C(4) – C(5) → σ* C(4) – H(10)	0.52	2.2
σ C(4) – C(5) → σ* C(5) – H(13)	0.52	2.2
σ C(4) – H(10) → σ* C(1) – C(5)	1.55	6.5

σ C(4) – H(10) → σ* O(2) – C(3)	2.10	8.8
σ C(4) – H(11) → σ* C(3) – H(8)	2.00	8.4
σ C(4) – H(11) → σ* C(3) – H(9)	0.61	2.6
σ C(4) – H(11) → σ* C(5) – H(12)	2.36	9.9
σ C(5) – H(12) → σ* C(1) – H(6)	2.00	8.4
σ C(5) – H(12) → σ* C(1) – H(7)	0.61	2.6
σ C(5) – H(12) → σ* C(4) – H(11)	2.36	9.9
σ C(5) – H(13) → σ* C(1) – O(2)	2.10	8.8
σ C(5) – H(13) → σ* C(3) – C(4)	1.55	6.5

[a] See Figure 1 for atoms numbering.
[b] E(2) means energy of hyper-conjugative interactions.

3.4. Molecular electrostatic potential (MEP)

The MEP which is a plot of electrostatic potential mapped into the constant electron density surface. The importance of MEP lies in the fact that it simultaneously display molecuar size, shape as well as positive, negative and neutral electrotatic potential regions in terms of color grading and is very useful in research of molecular structure with its physiochemical property relationship.

The different values of the electrostatic potential at the surface are represented by different colors; red represents regions of the most negative electrostatic potential, blue represents regions of the most positive electrostatic potential and green represents region of zero potential. Potential decreases in the trend of red < orange < yellow < green < blue. Figure 3a shows the MEP plot for the title compound calcuated by DFT/B3LYP method with 6-311++G(2d,2p) basis set using the computer software GaussView 6.0 [11]. This figure provides a visual representation of the chemically active sites and comparative reactivity of atoms. From the MEP it is evident that the negative charge covers the C–O–C group. The value of the electrostatic potential is largely responsible for the binding of a substrate to its receptor binding sites since the receptor and the corresponding logands recognize each other at their molecular surface.

3.5. Frontier molecular orbitals

The molecular orbital (MO) is a very important concept in quant um chemistry, being extensively employed to describe the chemical behavior. The highest occupied molecular orbital HOMO and lower unoccupied molecular orbital LUMO are the two most important molecular orbitals in a molecule as both are used to describe various chemical properties such as reactivity and kinetics [19]. These orbitals are known by the name frontier orbitals, they lie at the outermost boundaries of the electrons of the molecules. Both the HOMO and LUMO are the main orbitals that take part in the chemical stability. The HOMO represents the ability to donate an electron, LUMO as an electron acceptor represents the ability to obtain an electron. The difference of the energies of the HOMO and LUMO is a measure of the excitability of the molecule, the smaller the energy, more easily it can be excited and vice versa. The positive and negative phases are represented in red and green color, respectively. The plots reveal that the HOMO is primarily composed of O(2), C(1) and C(3) the corresponding to the aromatic ring. The LUMO is spread over the entire molecule excepy C–O–C group.

Table 4. HOMO-LUMO gap of Tetrahydrofuran by B3LYP/6-311++G(2d,2p) method

Molecular parameters	B3LYP/6-311++G(2d,2p) (1 a.u $\cong$ 27.211 eV)	
	(a.u)	(eV)
HOMO energy	-0.251	-6.830
LUMO energy	- 0.010	-0.272
Forntier orbital energy gap ($\Delta E_{HOMO\text{-}LUMO}$)	0.241	6.558

The energy value of HOMO and LUMO molecular orbitals with the corresponding HOMO-LUMO energy gap is show in Figue 3b. The HOMO-LUMO energy gap value is predicted 6.558 eV (Table 4). This value explains the eventual charge transfer interaction with the molecule, which influences the biological activity of the compound. The relatively high value of $\Delta E_{HOMO\text{-}LUMO}$ indicates that the title compound presents high chemical stablity and it has low reactivity.
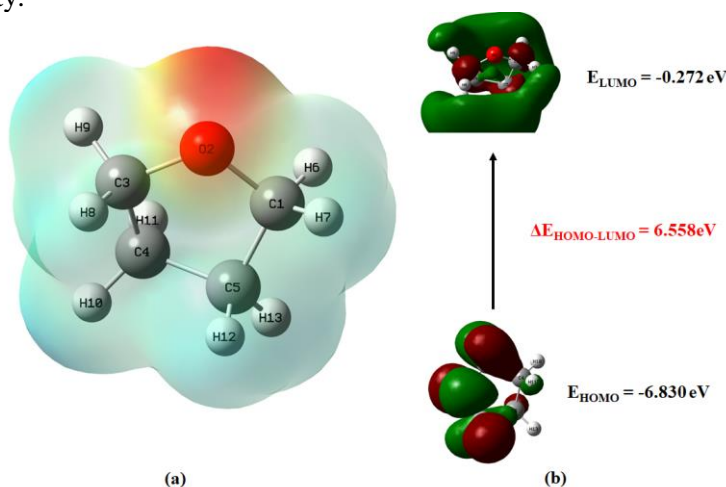

Figure 3. (a) Molecular electrostatic potential (MEP) map;
(b) $\Delta E_{HOMO\text{-}LUMO}$ energy gap for Tetrahydrofuran calculated at B3LYP/6-311++G(2d,2p) level.

4. CONCLUSION

A complete structural, vibrational investigation along with MEP, NBO and HOMO-LUMO analysis of Tetrahydrofuran (THF) have been carried out with DFT/B3LYP method using 6-311++G(2d,2p) basis sets. The vibrational spectra have been recorded and completely analyzed. The molecular geometry parameters, bond lengths and bond angles calculated with different methods and basis sets agreed well with the experimental values. The MEP exhibits the visual representation of the chemically active sites and comparative reactivity of atoms. The HOMO-LUMO energy gap is calculated to be 6.558 eV. This value explains the eventual charge transfer interaction with the molecule, which influences the boplogical activity of the compound. The relatively high value of $\Delta E_{HOMO\text{-}LUMO}$ indicates that the title compound presents high chemical stability and it has low reactivity. From this research results will be the premise of the next research on phase diagrams of tetrahydrofuran + water, as a co-solvent of THF to modify the phase behavior of THF-water and the hydrogen bond interaction in THF-water complex. It would be interesting to compare the theoretical binding energy values if such hydrogen bonded complex can be experimentally detected.

REFERENCES

1. Najeeb, H. N. - Density functional theory and semi-empirical investigations of amino tetrahydrofuran molecules, Phys. Mater. Chem **1** (2) (2013) 21-26.

2. David, W.I.F., & Ibberson, R.M. - A reinvestigation of the structure of tetrahydrofuran by high-resolution neutron powder diffraction, Acta Crystallographica Section C: Crystal Structure Communications **48** (2) (1992) 301-303.

3. Cadioli, B., Gallinella, E., Coulombeau, C., Jobic, H., & Berthier, G. - Geometric structure and vibrational spectrum of tetrahydrofuran, The Journal of Physical Chemistry **97** (30) (1993) 7844-7856.

4. Dwivedi, A., Baboo, V., & Bajpai, A. - Fukui function analysis and optical, electronic, and vibrational properties of tetrahydrofuran and its derivatives: A complete quantum chemical study, Journal of Theoretical Chemistry (2015) 345234.

5. Becke, A. D. - Density-functional exchange-energy approximation with correct asymptotic behavior, Physical review A **38** (6) (1988) 3098.

6. Lee, C., Yang, W., & Parr, R. G. - Development of the Colle-Salvetti correlation-energy formula into a functional of the electron density, Physical Review B **37** (2) (1988) 785.

7. Kendall, R. A., Dunning Jr, T. H., & Harrison, R. J. - Electron affinities of the first-row atoms revisited. Systematic basis sets and wave functions, The Journal of Chemical Physics **96** (9) (1992) 6796-6806.

8. Glendening, E. D., Badenhoop, J. K., Reed, A. E., Carpenter, J. E., Bohmann, J. A., Morales, C. M., & Weinhold, F. - Theoretical Chemistry Institute: University of Wisconsin, Madison, WI, 2001NBO **5** (2001).

9. Politzer, P., Laurence, P. R., & Jayasuriya, K. - Molecular electrostatic potentials: an effective tool for the elucidation of biochemical phenomena, Environmental Health Perspectives **61** (1985) 191-202.

10. Frisch, M. J., Trucks, G. W., Schlegel, H. B., Scuseria, G. E., Robb, M., Cheeseman, J. R., & Fox, D. J. - Gaussian Inc. Wallingford Ct. (2009).

11. Dennington, R., Keith, T., & Millam, J. - GaussView, version 6 (2016).

12. http://webbook.nist.gov/chemistry

13. Sahu, P. K., Chaudhari, A., & Lee, S. L. - Theoretical investigation for the hydrogen bond interaction in THF–water complex, Chemical Physics Letters **386** (4-6) (2004) 351-355.

14. Jamroz, M. H. - Vibrational energy distribution analysis VEDA **4** (2004).

15. Lin-Vien, D., Colthup, N. B., Fateley, W. G., & Grasselli, J. G. - The handbook of infrared and Raman characteristic frequencies of organic molecules, Elsevier (1991).

16. Silverstein, R. M., & Bassler, G. C. - Spectrometric identification of organic compounds, Journal of Chemical Education **39** (11) (1962) 546.

17. Mohan, J. - Organic spectroscopy: principles and applications, Alpha Science Int'l Ltd. (2004).

18. Glendening, E.D., Reed, A.E., Carpenter, J.E. and Weinhold, F., NBO (version 3.1) - Theoretical Chemistry Institute, University of Wisconsin: Madison, WI (1996).

19. Zhang, G., & Musgrave, C. B. - Comparison of DFT methods for molecular orbital eigenvalue calculations, The Journal of Physical Chemistry A **111** (8) (2007) 1554-1561.

TÓM TẮT

PHÂN TÍCH HÌNH HỌC, PHỔ DAO ĐỘNG, NBO, MEP VÀ HOMO-LUMO CỦA TETRAHYDROFURAN (THF) DỰA TRÊN TÍNH TOÁN DFT

Trương Tấn Trung[1*], Nguyễn Phương Đông[2],
Lại Thị Hiền[1], Lê Thị Thu Thủy[1]
[1]*Trường Đại học Công nghệ Đồng Nai*
[2]*Trường Đại học Soongsil, Hàn Quốc*
Email: truongtantrung@dntu.edu.vn

Trong bài báo này, hình học tối ưu, phổ dao động được tính toán bằng thuyết phiếm hàm mật độ DFT (Density Functional Theoretical) tại mức lý thuyết B3LYP với bộ cơ sở 6-311++G(2d,2p). Các dao động cơ bản được ấn định trên cơ sở sự phân bố năng lượng thế năng PED (potential energy distribution) của các dao động được tính toán bằng chương trình VEDA. Ngoài ra, các tính toán obital phân tử như obital liên kết thích hợp NBO (Nutural Bond Orbital), năng lượng HOMO-LUMO và thế năng tĩnh điện MEP (Molecular Electrostatic Potential) cũng được thực hiện cùng mức lý thuyết DFT. Năng lượng tương tác nhiễu loạn bậc 2 (E(2)) (second-order perturbation interaction energy) tương tác giữa cho/nhận điện tử (donor/aceeptor electron) được xác định bằng phân tích NBO. Khoảng cách năng lượng HOMO–LUMO ($\Delta E_{HOMO-LUMO}$) là 6.558 eV. Một số dao động cơ bản như dao động dãn/uốn C–H, dao động xoắn của phân tử cũng được phân tích và so sánh với dữ liệu báo cáo trước đây và dữ liệu thực nghiệm.

Từ khóa: Tetrahydrofuran, DFT, NBO, MEP, HOMO-LUMO.